Journal of
Applied Crystallography
ISSN 0021-8898

Received 16 August 2006
Accepted 18 December 2006

Discrepancy in determination of χ parameters by melting point depression *versus* small-angle neutron scattering in blends of deuterated polycarbonate and isotactic poly(methyl methacrylate)

Thein Kyu,* Rushikesh A. Matkar, Dong Soo Lim and Chechian Ko

Department of Polymer Engineering, University of Akron, Akron, OH-44325, USA. Correspondence e-mail: tkyu@uakron.edu

The discrepancy in the χ interaction parameters of deuterated polycarbonate/isotactic poly(methyl methacrylate) blends as determined by the melting point depression approach and the small-angle scattering technique is reported. We have modified the Flory diluent theory by removing the inherent assumption of complete rejection of the solvent from the crystal solid by taking into consideration the crystal–amorphous, amorphous–crystal, and crystal–crystal interactions. The discrepancy in χ values obtained by the two methods is discussed.

© 2007 International Union of Crystallography
Printed in Singapore – all rights reserved

1. Introduction

The tacticity of poly(methyl methacrylate) (PMMA) isomers has been recognized to exert profound effects on its miscibility with other polymers (Schurer *et al.*, 1975; Silvestre *et al.*, 1987). In our laboratory, blends of polycarbonate (PC)/PMMA isomers have been explored as a means of controlling the transparency of their blend films and the refractive index gradient (Lim & Kyu, 1991). It was found that PC/syndiotactic poly(methyl methacrylate) (sPMMA) and PC/atactic poly(methyl methacrylate) (aPMMA) can be characterized as partially miscible with a cloud point phase diagram reminiscent of a lower critical solution temperature (LCST). The proximity of the aforementioned LCST to the glass transition temperatures of the constituents of the PC/PMMA blends, coupled with slow mutual diffusion of the polymer chains, impeded the exploration of the miscibility of PC/aPMMA and PC/sPMMA blends near their glass transition temperatures (T_g) by conventional techniques such as light scattering or optical microcopy. However, thermal reversibility of the LCST phase behavior could not be established for either of these blends. Hence, we shall focus on small-angle neutron scattering (SANS) experiments of deuterated polycarbonate (dPC)/isotactic poly(methyl methacrylate) (iPMMA) blends.

In the present paper, SANS has been employed for the determination of the χ interaction parameter in the vicinity of the coexistence lines of the dPC/iPMMA blend using the Ornstein–Zernike approach (Kirste *et al.*, 1975). The uniqueness of the present PC/iPMMA blend is that both constituents can crystallize upon annealing above their glass transition temperatures. The melting point depression of PC was analyzed in the framework of the polymer diluent theory (Flory, 1953; Nishi & Wang, 1975). The χ value of the PC/iPMMA blend obtained by the Flory diluent analysis was subsequently compared with that obtained by SANS.

2. Materials and methods

The deuterated PC (dPC) was obtained from Dr Steve Smith of the Procter & Gamble Company. The as-received dPC was purified by dissolving in tetrahydrofuran (thf) at a concentration of 2 wt% and filtered twice using a microfilter having a pore diameter of 0.45 µm. The number-average (M_n) and weight-average (M_w) molecular weights of dPC were 23 400 and 48 800 g mol^{-1}, respectively, and the corresponding M_n and M_w values of the regular PC were 21 500 and 58 000 g mol^{-1}, respectively. Its counterpart iPMMA, denoted by iPMMA-1, was purchased from Polymer Laboratories, Inc. It had a broad molecular weight distribution ($M_w/M_n = 3.85$), so was further fractionated into various narrow molecular weight fractions *via* precipitation from chloroform solution. The molecular weights of these iPMMA fractions were designated by numbers indicating the weight-average molecular weight in units of thousands. The molecular weight distributions are in the range of 1.2 to 1.4.

Blends of dPC/iPMMA were prepared by dissolving dPC and iPMMA in thf and then co-precipitating the solution in heptane. The precipitates were dried in a vacuum oven for 2 days at about 353 K. Samples for SANS experiments were compression molded in a hot press at 523 K for 480 s under a pressure of 2 GPa into a disc having a diameter of 15 mm. The molded discs were transparent and free from bubbles to the naked eye.

SANS measurements were performed at the Koehler 30 m SANS facility at the Oak Ridge National Laboratory (ORNL), Tennessee, USA. The detector size was 640 × 640 mm with a neutron wavelength $\lambda = 0.475$ nm. The sample-to-camera distance was 16.23 m. This gave the magnitude of the scattering vector, q, in the range 0.03–0.36 nm^{-1}, where q is defined as $q = (4\pi/\lambda)\sin(\theta/2)$, where θ is the scattering angle.

Blends of the PC/iPMMA show the development of crystals in both PC and iPMMA when annealed at 383 K for a few days. Differential scanning calorimetry (DSC) scans were acquired on these annealed crystalline blends using a DuPont differential scanning calorimeter (model 910) equipped with a temperature controller (model 9900). The DSC heating rate was 10 K min^{-1} unless indicated otherwise.

3. Results and discussion

3.1. Effect of molecular weight on interaction parameter and miscibility

In Fig. 1(a) are shown the neutron scattering cross sections of the 50/50 dPC/iPMMA blends at 423 K for various molecular-weight

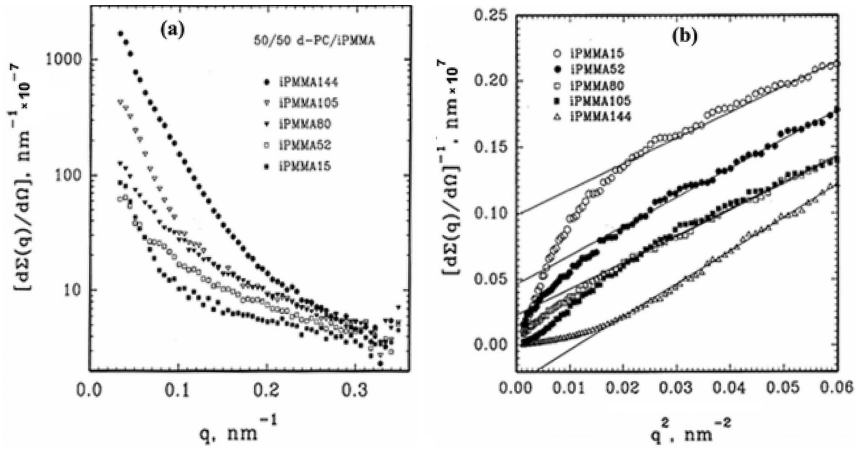

Figure 1
(*a*) The molecular weight dependence of the neutron cross section *versus q* plots for various dPC/iPMMA blends at 423 K having various molecular weight fractions indicated by the numbers in units of thousands, and (*b*) the Ornstein–Zernike plots for the determination of the correlation lengths for various weight-average molecular weight fractions.

fractions of iPMMA, with the numbers indicating the units in thousands. The SANS intensities decay monotonically with increasing scattering angle or q. As can be expected for a miscible blend, there is no identifiable scattering peak. The monotonically decreasing trend of the scattering intensity with q becomes more pronounced with increasing molecular weight of iPMMA, indicating that the miscibility of the dPC/iPMMA blend is diminished as the molecular weight of one constituent increases. In the highest molecular weight sample, dPC/iPMMA-144 (*i.e.*, weight-average molecular weight of 144 000), the scattering is very strong, which in turns suggests that the system may be approaching the phase separation limit. The reduction of blend miscibility with increasing molecular weight is consistent with the prediction by the classical Flory–Huggins (FH) theory (Flory, 1953), in that the mixing entropy is reduced with longer chain lengths, giving rise to an unfavorable entropic contribution to the miscibility. The SANS data for the above miscible blends were analyzed in the context of the Ornstein–Zernike approach (*e.g.*, see Shibayama *et al.*, 1985) given by:

$$[\mathrm{d}\Sigma(q)/\mathrm{d}\Omega]^{-1} = [\mathrm{d}\Sigma(0)/\mathrm{d}\Omega]^{-1} + \xi^2 q^2 [\mathrm{d}\Sigma(0)/\mathrm{d}\Omega]^{-1}, \qquad (1)$$

where $[\mathrm{d}\Sigma(0)/\mathrm{d}\Omega]^{-1} = (2/k_\mathrm{N}V_0)(\chi_\mathrm{s} - \chi)$ with V_0 being the reference volume and $\xi^2 = (\bar{b}^2/36)[\phi_1\phi_2(\chi_\mathrm{s} - \chi)]^{-1}$ with ϕ_1 and ϕ_2 being volume fractions of the constituents. The interaction parameter at a given temperature is given by χ and the subscript s signifies χ at the spinodal point. The constant k_N is defined as $k_\mathrm{N} = N_0(a_1/V_1 - a_2/V_2)^2$ in which N_0 is the Avogadro number, a_i are the scattering lengths per segment of the component i, ξ is the correlation length, and $\bar{b}^2$ is the mean square average of the segment lengths given as

$$\frac{\bar{b}^2}{V_0} = \left[\phi_1\phi_2\left(\frac{\langle r_1\rangle_z b_1^2}{\langle r_1\rangle_\mathrm{w} V_1\phi_1} + \frac{\langle r_2\rangle_z b_2^2}{\langle r_2\rangle_\mathrm{w} V_2\phi_2}\right)\right], \qquad (2)$$

where $\langle r_i\rangle_z$ and $\langle r_i\rangle_\mathrm{w}$ are the z-average and weight-average molecular weights of the components, respectively, and V_i are the molar volumes of the constituents.

There is a significant departure from the linear slope in the plots at very small q due to the strong scattering persisting in the neat dPC despite the repeated purification (at least twice) (Fig. 1*b*). The excess SANS as seen here for all the dPC/iPMMA blends at small scattering angles leading to the deviations from linearity has been reported in the literature for a number of miscible blends and has been attributed to several sources, including uneven quenching, cavitation (Murray, Gilmer & Stein, 1985; Koch & Strobl, 1990), or residual phase separation (Clark *et al.*, 1993).

In the present study, the analysis was carried out with emphasis on the larger q values. In accordance with the above Ornstein–Zernike equation, the correlation distance ξ and the χ parameter were determined from the linear slope at larger q and the intercept at $q = 0$ (Fig. 1*b*). It should be noted that the parameter obtained from this Ornstein–Zernike approach may be considered as equivalent to the χ parameter in the FH theory as it is directly related to the enthalpic contribution of the free energy of mixing at the critical point. The values of parameters thus estimated are plotted in Fig. 2 as a function of molecular weight. They vary from −0.04 to −0.008 in order of ascending molecular weight.

3.2. Determination of χ parameter based on melting point depression

Blends of PC and stereospecific PMMA isomers are capable of forming crystals upon exposure to solvent or by annealing. We annealed the PC/iPMMA blends to induce crystals in these components in order to determine the polymer–polymer interaction in accordance with the melting point depression analysis (Flory, 1949).

In view of the non-equilibrium nature of polymer crystallization, the melting temperature (T_m) and crystallinity is expected to change with annealing time. Thus, it is important to establish the experimental conditions such as annealing time and temperature. First, we selected 383 K as the annealing temperature, because it is the onset point of the glass transition for the 90/10 PC/iPMMA blend (*i.e.*, the highest PC concentration studied) and is significantly lower than the degradation temperature of iPMMA. Upon annealing at 383 K for 1 day, thermally induced crystallization of neat iPMMA took place. When blends of PC/iPMMA were annealed at 383 K for 3 days, both PC and iPMMA crystallized to the fullest extent at intermediate compositions as depicted in the DSC thermograms (Fig. 3); that is to say the crystallinity of PC in the blends gradually increases up to 3 days of annealing, but it levels off thereafter. The crystallization of

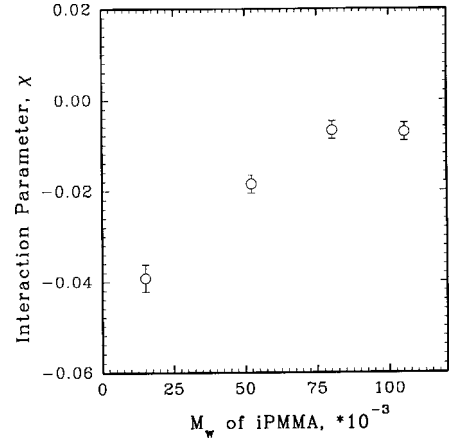

Figure 2
The amorphous–amorphous interaction parameters of dPC/iPMMA blends as a function of molecular weights of iPMMA from the SANS measurements.

PC in the blend may be attributed to the enhanced mobility of PC chains afforded by the surrounding iPMMA. The present observation is consistent with the reports for the blends of PC with other constituents such as poly(ε-caprolactone) or poly(hexamethylene sebacate) (Nasser *et al.*, 1979). The crystallization rate of PC is seemingly expedited upon blending with low molecular weight plasticizers.

Fig. 3 illustrates the DSC thermograms of various PC/iPMMA blends showing the depression of the melting point of the PC crystals with increasing iPMMA. However, iPMMA shows little or no change in the melting temperature, which may be attributed to the restricted mobility imposed by the solid crystalline PC, which serves as physical crosslinks, and thus no plasticizing of iPMMA crystals occurs. Since the pure PC cannot form any crystals by simply annealing, crystallization was induced by exposing PC to MMA monomer, which is generally known as solvent-induced crystallization (O'Reilly *et al.*, 1964). The melting point of pure PC crystals thus measured by DSC was 596 K, which was regarded as T_m. In principle, it is desirable to determine the equilibrium melting temperatures at $T_m = T_c$ (*i.e.*, crystallization temperature) (Hoffman & Weeks, 1962), but it is extremely difficult for the present PC/iPMMA system due to the slow crystallizing habit of the constituents. Moreover, prolonged annealing beyond 5 days results in degradation of the polymers. Assuming the measured melting points of PC crystals in the blends are sufficiently close to their respective equilibrium melting temperatures, the melting point depression of PC may be analyzed in accordance with the analytical expression of the Flory diluent theory (Flory, 1949) as depicted in Fig. 4. Using the value of the heat of fusion of PC crystals, ΔH_{PC} = 32.4 kJ mol^{-1} (Adams *et al.*, 1976), the value of χ was estimated to be −0.15 at 573 K, suggestive of the miscible character.

However, this χ value of −0.15 from the melting point depression is significantly larger than those obtained by SANS of the PC/iPMMA blends, *i.e.*, −0.04 to −0.008. Such discrepancy has been reported for numerous blends (Canalda *et al.*, 1995), but there is no critical challenge as to why such a large discrepancy exists for the melting-temperature depression approach *versus* neutron scattering. Secondly, the meaning of the FH parameter based on the melting point depression is vague (Nishi & Wang, 1975); that is to say, whether it represents the amorphous–amorphous interaction as in the case of SANS or the crystal–amorphous interaction. The problem seems to reside in the inherent assumption of the Flory diluent theory that solvent is completely rejected from the polymer crystal, *i.e.*, the chemical potential of the liquid solution was equated to that of the pure polymer crystal. This complete immiscibility assumption is the source of the major deficiency in the original Flory diluent theory, which is incapable of explaining the solidus line of the phase diagram (Burghardt, 1989; Konigsveld & Stockmayer, 2001).

3.3. Modification of the Flory diluent theory for crystalline polymer blends

We have modified the Flory diluent theory for a crystalline–amorphous polymer blend by taking into consideration the solid solution phase (Matkar & Kyu, 2006*a*) which has been known to exist in other binary systems such as metal alloys, organic molecular solutions, and crystal–liquid crystal mixtures (Dayal *et al.*, 2006). A unified theoretical model (Matkar & Kyu, 2006*b*) has been developed in the framework of the phase field model of solidification involving the Landau-type double-well potential pertaining to the first order solid–liquid phase transition (Xu *et al.*, 2005) coupled with the FH free energy for liquid–liquid demixing (Flory, 1953).

The total free energy density of mixing of a binary crystalline polymer blend may be expressed as the weighted sum of the free energy density pertaining to crystal solidification of the crystalline constituent with its volume fraction (ϕ) and the free energy of liquid–liquid mixing as described by the FH theory of isotropic mixing with the addition of the anisotropic interaction terms including crystal–amorphous, amorphous–crystal, and crystal–crystal mixing:

$$f(\psi_1, \psi_2, \phi_1, \phi_2) = \phi_1 f(\psi_1) + \phi_2 f(\psi_2) + \frac{\phi_1}{r_1}\ln\phi_1 + \frac{\phi_2}{r_2}\ln\phi_2 + \left[\chi_{aa} + \left(\chi_{ca}\psi_1^2 - 2\chi_{cc}\psi_1\psi_2 + \chi_{ac}\psi_2^2\right)\right]\phi_1\phi_2. \quad (3)$$

The first two terms, $\phi_1 f(\psi_1) + \phi_2 f(\psi_2)$, represent the Landau-type free energy of crystal solidification of each component pertaining to the crystal order parameters of the constituent i, ψ_i, in which the

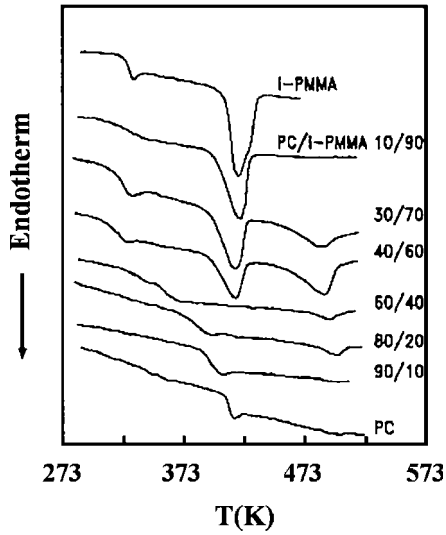

Figure 3
DSC thermograms of PC/iPMMA-1 blends showing the melting transitions of the intermediate compositions of the PC/iPMMA blends upon annealing at 383 K for 3 days.

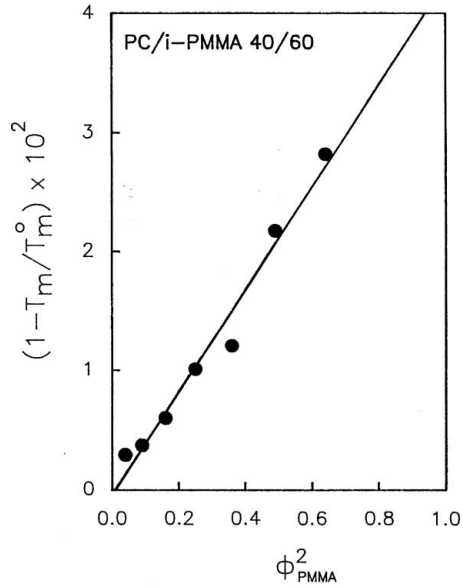

Figure 4
The analysis of the melting point depression based on the original Flory diluent theory of dPC/iPMMA-1, *i.e.*, a $(1 - T_m/T_m^0)$ *versus* ϕ^2 plot from which χ is estimated to be −0.15.

individual free energy of the constituents is weighted by the respective volume fractions to guarantee that these potentials vanish at the extreme limits of zero crystallinity or if a component is not crystallizable. The second two terms, $(\phi_1/r_1)\ln\phi_1 + (\phi_2/r_2)\ln\phi_2$, represent the entropic terms of the constituents in the liquid or melt state with r_1 and r_2 being the statistical segment lengths of the constituent polymers. The last term (in square brackets) represents the enthalpic contribution, which corresponds to the amorphous–amorphous interaction parameter of FH that characterizes the stability of the liquid phase, and the anisotropic interactions such as the repulsive crystal–amorphous and amorphous–crystal interactions in forming separate crystals, and the attractive crystal–crystal interaction that favors the formation of co-crystals.

The free energy density of crystal solidification pertaining to the crystal phase order parameter (ψ_i) may be described in the context of the Landau-type asymmetric potential, *viz*.

$$f(\psi_i) = \frac{F(\psi_i)}{k_B T} = W_i \int_0^{\psi_i} \psi_i(\psi_i - \zeta_i)(\psi_i - \zeta_{i,0})\,\mathrm{d}\psi_i$$
$$= W_i\left[\frac{\zeta_i(T)\zeta_{i,0}(T_{i,m})}{2}\psi_i^2 - \frac{\zeta_i(T) + \zeta_{i,0}(T_{i,m})}{3}\psi_i^3 + \frac{1}{4}\psi_i^4\right], \quad (4)$$

where k_B is the Boltzmann constant and T is the absolute temperature. The coefficients of the Landau free energy expansion based on the crystal order parameter (ψ_i) of the constituents are treated as temperature dependent in polymer crystallization to account for the imperfect nature of polymer crystals. These crystal phase order parameters are defined as the ratio of the lamellar thickness (l_i) to the lamellar thickness of a perfect polymer crystal (l_i^0), *i.e.*, $\psi_i = l_i/l_i^0$, to represent the one-dimensional crystallinity (Xu *et al.*, 2005). W_i is a dimensionless coefficient representing the energy penalty, ζ_i represents the crystal order parameter at the peak position of the barrier, and $\zeta_{i,0}$ represents the stable potential well for the system to equilibrate during solidification.

By definition, the crystal order parameter ψ_1 is the linear crystallinity of component 1 and thus the product with its volume fraction $(\phi_1\psi_1)$ corresponds to the bulk crystallinity in the blend. On the other hand, the product $(\phi_2\psi_1)$ implies the amount of amorphous material interacting with the crystalline phase, and hence the term $\chi_{ca}(\phi_1\psi_1)(\phi_2\psi_1)$ signifies the repulsive crystal–amorphous interaction. The same argument may be made for the second crystalline component, *i.e.* $\chi_{ac}(\phi_2\psi_2)(\phi_1\psi_2)$, representing the amorphous–crystal interaction. By the same token, the cross-interaction term, $\chi_{cc}(\phi_1\psi_1)(\phi_2\psi_2)$, may be interpreted as the crystal–crystal interaction of the co-crystals (Matkar & Kyu, 2006*b*).

The anisotropic interactions, such as crystal solid–amorphous liquid or amorphous liquid–crystal solid interactions, may be symbolized by χ_{ca} and χ_{ac}, respectively. These anisotropic interactions of separate crystals and co-crystals are complimentary to χ_{aa}, representing the isotropic interaction of amorphous materials. Moreover, these crystal–amorphous interaction parameters may be estimated from the heat of fusions of the crystals, *i.e.*, $\chi_{ca} \propto W_1 = 6(\Delta H_1^c/k_B T)(1 - T/T_{1,m})/(0.5 - \zeta_1)$ and $\chi_{ac} \propto W_2 = 6(\Delta H_2^c/k_B T)(1 - T/T_{2,m})/(0.5 - \zeta_2)$, where ΔH_1^c and ΔH_2^c are enthalpies of crystallization of components 1 and 2, respectively. Furthermore, the crystal–crystal interaction may be expressed as a geometric mean of the crystal–amorphous and amorphous–crystal interactions to account for the non-ideal rule of the crystalline mixture, *i.e.*, $\chi_{cc} = c_w[(\chi_{ca})^{1/2}(\chi_{ac})^{1/2}]$, in which c_w represents the anisotropic interaction parameter, which signifies any departure from ideality (Matkar & Kyu, 2006*b*).

In the present case, PC and iPMMA show no indication of co-crystallization, thus c_w may be taken as zero or negligibly small, *i.e.* 0.001 in the present case. Fig. 5 shows the melting points of PC and iPMMA in which the depression of the melting point of the PC crystals is evident. Although the experimental melting temperatures of PC and its blends were not determined at the equilibrium conditions, the relative trend is not expected to change significantly. We have solved self-consistently equations (3) and (4) by minimizing the free energies with respect to the crystal order parameters ψ_1 and ψ_2 to determine the solid crystal–liquid (melt) transition lines of the constituents, and subsequently determined the liquidus and solidus lines by equating the chemical potentials of each polymer crystal. The crystal–amorphous interaction parameters of PC and iPMMA were estimated based on the heat of fusions of PC and iPMMA to be 32.4 kJ mol^{-1} (Adams *et al.*, 1976) and 4.6 kJ mol^{-1} (Kusy, 1976), respectively, which gave χ_{ca} and χ_{ac} as 0.79 and 0.13 at their crystal–melt transition temperatures. The calculation gave the amorphous–amorphous interaction parameter χ_{aa} as -0.018, which is now consistent with the value of -0.02 obtained by neutron scattering experiments at 495 K. The self-consistent solutions reveal that the liquidus line coincided with the experimental melting transitions while the solidus line is located right on the pure PC crystal axis. The melting point of iPMMA shows little or no movement with the addition of PC, which is not surprising in view of the solidification of PC crystals and the fact that the amorphous PC chains are close to their glass transitions. The close match between the melting transition points of PC/iPMMA with the calculated liquidus line implies the importance of taking into consideration the crystal–amorphous interaction of PC/iPMMA in addition to the amorphous–amorphous interaction. It may be inferred that the overestimation of the χ parameter based on the melting point depression relative to the neutron scattering may be attributed to the poor assumption in the original Flory diluent theory (Flory, 1953), *i.e.*, the complete rejection of the solvent from the crystalline solid. It should be emphasized that the proposed modification of the FH theory can predict numerous phase diagrams of binary crystal blends, encompassing eutectic, peritectic, and azeotrope phase diagrams bound by the solidus and liquidus coexistence lines (Matkar & Kyu, 2006*a*,*b*).

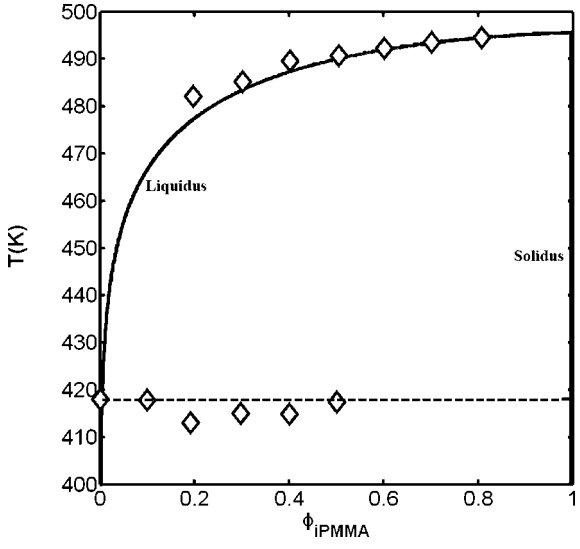

Figure 5
Comparison of the observed melting points with the liquidus and solidus lines of the self-consistent solutions that gives the χ_{aa} value of -0.018 based on $\chi_{ca} = 0.79$ and $\chi_{ac} = 0.13$.

4. Conclusions

The present paper demonstrated that the Flory diluent theory overestimated the χ interaction parameter relative to that obtained by neutron scattering experiments. The removal of the complete immiscibility assumption of the original Flory diluent theory allows the proper establishment of binary crystal phase diagrams which are now consistent with those of binary metal alloys, molecular crystals, and liquid crystals. Moreover, with this modification, the χ parameter becomes comparable to those obtained by the melting point depression and neutron scattering experiments. The present study also points to the fact that the crystal–amorphous interactions must be considered in order to describe the complete phase diagrams of the binary crystalline polymer blends and also to cover all coexistences regions bound by the solidus and liquidus lines.

The authors express their sincere thanks to Dr Steve Smith of the Procter & Gamble Company for supplying deuterated PC and Drs J. S. Lin and G. D. Wignall of Oak Ridge National Laboratory for their professional help in conducting the SANS experiments. The present study is made possible by partial support from the National Science Foundation through grant No. DMR-0514942.

References

Adams, G. A., Hay, J. N., Parsons, I. W. & Haward, R. N. (1976). *Polymer*, **17**, 51–57.
Bates, F. S., Dierker, S. B. & Wignall, G. D. (1986). *Macromolecules*, **19**, 1938–1945.
Beaucage, G., Stein, R. S., Hashimoto, T. & Hasegawa, H. (1991). *Macromolecules*, **24**, 3443–3448.
Burghardt, W. R. (1989). *Macromolecules*, **22**, 2482–2486.
Butzbach, G. D. & Wendorff, J. H. (1991). *Polymer*, **32**, 1155–1159.
Canalda, J. C., Hoffmann, Th. & Martinez-Salazar, J. (1995). *Polymer*, **36**, 981–985.
Clark, N. G., Fernandez, M. L., Tomlins, P. E. & Higgins, J. S. (1993). *Macromolecules*, **26**, 5897–5907.
Dayal, P., Matkar, R. A. & Kyu, T. (2006). *J. Chem. Phys.* **124**, 224902/1–7.
Flory, P. J. (1949). *J. Chem. Phys.* **17**, 223–240.
Flory, P. J. (1953). *Principles of Polymer Chemistry*. Ithaca, New York: Cornell University Press.
Hoffman, J. D. & Weeks, J. J. (1962). *J. Res. Natl Bur. Stand. A*, **66**, 13–28.
Lim, D. S. & Kyu, T. (1991). *Macromolecules*, **24**, 3645–3650.
Kirste, R. G., Kruse, W. A. & Ibel, K. (1975). *Polymer*, **16**, 120–124.
Koch, T. & Strobl, G. R. (1990). *J. Polym. Sci. Polym. Phys. Ed.* **28**, 343–353.
Konigsveld, R. & Stockmayer, W. H. (2001). *Polymer Phase Diagrams*. Oxford University Press.
Kusy, R. P. (1976). *J. Polym. Sci. Polym. Chem. Ed.* **14**, 1527–1536.
Kyu, T., Ko, C. C., Lim, D. S., Smith, S. & Noda, I. (1993). *J. Polym. Sci. B Polym. Phys.* **31**, 1641–1648.
Matkar, R. A. & Kyu, T. (2006*a*). *J. Phys. Chem. B*, **110**, 12728–12732.
Matkar, R. A. & Kyu, T. (2006*b*). *J. Phys. Chem. B*, **110**, 16059–16065.
Murray, C. T., Gilmer, J. W. & Stein, R. S. (1985). *Macromolecules*, **18**, 996–1002.
Nasser, T. R., Paul, D. R. & Barlow, J. W. (1979). *J. Appl. Polym. Sci.* **23**, 85–99.
Nishi, T. & Wang, T. T. (1975). *Macromolecules*, **8**, 909–915.
O'Reilly, J. M., Karasz, F. E. & Bair, H. E. (1964). *J. Polym. Sci. C*, **6**, 109–115.
Schurer, J. W., de Boer, A. & Challa, G. (1975). *Polymer*, **16**, 201–204.
Shibayama, M., Yang, H., Stein, R. S. & Han, C. C. (1985). *Macromolecules*, **18**, 2179–2187.
Silvestre, C., Cimmino, S., Martuscelli, E., Karasz, F. E. & MacKnight, W. J. (1987). *Polymer*, **28**, 1190–1199.
Yang, H., Hadziioannou, G. & Stein, R. S. (1983). *J. Polym. Sci. B Polym. Phys.* **21**, 159–162.
Xu, H., Matkar, R. A. & Kyu, T. (2005). *Phys. Rev. E*, **72**, 011804/1–9.